Colloid Polym Sci 274:316–333 (1996)
© Steinkopff Verlag 1996

ORIGINAL CONTRIBUTION

K.M. McGrath
C.J. Drummond

Polymerisation of liquid crystalline phases in binary surfactant/water systems

Part 1. Allyldodecyldimethylammonium bromide and allyldidodecylmethylammonium bromide

Received: 9 March 1995
Accepted: 26 October 1995

K.M. McGrath[1]
Department of Applied Mathematics
Research School of Physical Sciences
and Engineering
The Australian National University
Canberra ACT 0200, Australia

[1]*Present address*:
Dr. K.M. McGrath (✉)
Department of Physics
Princeton University
P.O. Box 708
Princeton, New Jersey 08544, USA

C.J. Drummond
CSIRO Division of Chemicals and Polymers
Private Bag 10, Rosebank MDC
Clayton Victoria 3169, Australia

Abstract The binary phase behaviour of two potentially polymerisable quaternary ammonium surfactants in water has been investigated. Allyldodecyldimethylammonium bromide (ADAB) a single-chain surfactant displays a conventional phase progression upon increasing concentration. Whereas the double-chain analogue allyldidodecylmethylammonium bromide (ADDAB) forms two lamellar liquid crystalline phases built from surfactant bilayers, which transform via a first order phase transition. The formation of two distinct lamellar phases and their coexistence has been evidenced by optical microscopy, small-angle x-ray scattering and D_2O deuterium quadrupolar nuclear magnetic resonance spectroscopy. The lamellar phase formed at higher surfactant compositions is a normal lamellar phase (type L_α), consisting of bilayers which are on average parallel and flat. The lower compositional lamellar phase (type L_χ) in contrast may not be comprised of planar bilayers but rather aggregates having a high degree of curvature in comparison to those of the L_α phase. The presence of the allyl polymerisable moiety in the head group position of these surfactants has the effect of reducing the rigidity of the surfactant and increasing its solubility in comparison to non-polymerisable analogues. Polymerisation of the surfactants was attempted by using thermal and photochemical initiation in isotropic and self-assembled systems. Polymerisation occurred to approximately 30% for ADAB but did not occur for ADDAB. Where polymerisation did occur the polymer was incorporated into the monomer matrix by interweaving between the surfactant aggregates. The polymers had a molecular weight not greater than 8000 Daltons, independent of the monomer concentration of the original solution and type of polymerisation.

Key words Polymerisation – surfactant self-assembly – liquid crystals – allyldodecyldimethylammonium bromide – allyldidodecylmethylammonium bromide

Introduction

Amphiphilic molecules due to their hydrophilic/hydrophobic nature may be utilised in a wide range of applications. Despite this, the inherent instability of surfactant assemblages to perturbations (e.g. variations in temperature, composition and additives) does in fact limit their wider range of applicability. The "locking in" of the structure of mesophases either completely or partially (i.e.,

increasing their stability as a function of temperature, concentration and pressure) could lead to the development of new uses for surfactants.

Increasing the stability of the liquid crystalline phases may be accomplished in two ways, either via stabilisation or rigidification. Stabilisation may involve the addition of a component to the system or the surfactant itself may be polymerised prior to aggregation. Rigidification, in contrast, can only be achieved subsequent to surfactant self-assembly. Hence, it must involve polymerisation of one or more of the components in the system.

Polymerisation subsequent to surfactant self-assembly has been performed by a number of groups utilising different types of systems and reaction conditions [1–21]. Nevertheless, there are several complications involved in the polymerisation of surfactant lyotropic liquid crystalline phases, many of which are still not fully resolved, due to the lack of a complete picture of the mechanism of surfactant self-assembly. The approach adopted here was, therefore, to simplify the system as much as possible in an attempt to understand the chemical and physical processes involved during polymerisation.

One of the simplest and most widely studied polymerisable moieties is the allyl group, which is based on a single carbon–carbon double bond ($R–CH_2–CH=CH_2$). The allyl group was incorporated into the head group of a single- and a double-chain quaternary ammonium surfactant, yielding allyldodecyldimethylammonium bromide (ADAB, $CH_3–(CH_2)_{11}–N^+(CH_3)_2(CH_2–CH=CH_2)Br^-$) and allyldidodecylmethylammonium bromide (ADDAB, $(CH_3–(CH_2)_{11})_2–N^+(CH_3)(CH_2–CH=CH_2)Br^-$).

A single allyl polymerisable moiety was chosen, despite being known for its resistance to polymerisation (i.e., it is difficult to initiate and termination reactions are often favoured over propagation during polymerisation), because this group is the smallest polymerisable moiety available for use. Incorporation of this polymerisable moiety induces the minimal modification to the nature of the surfactant.

Addition of a polymerisable moiety into the head group of a surfactant will have an affect upon the surfactant's self-assembling properties. In the case of the allyl group, there will be an increase in the number of degrees of freedom for the head group of the surfactants. This will lead to surfactant molecules having different head group configurations, and in affect the surfactant volume and head group area will fluctuate to a large extent between the molecules. This increased flexibility will alter the inherent rigidity of the surfactant and consequently affect the surfactant's self-assembly. The allyl group, with its carbon–carbon double bond, also increases the overall hydrophilicity of the head group. Therefore, by direct comparison with analogous non-polymerisable surfactants (dodecyltrimethylammonium bromide (DTAB, $CH_3–(CH_2)_{11}–N^+(CH_3)_3Br^-$) [22–26] in the case of ADAB and didodecyldimethylammonium bromide (DDAB, $(CH_3–(CH_2)_{11})_2–N^+(CH_3)_2Br^-$) [27–33] in the case of ADDAB, where the allyl group has replaced the small hydrophobic methyl group in both surfactants) information on the exact affect that this addition will have upon surfactant self-assembly can be obtained and used to predict the behaviour of new surfactants which contain this polymerisable moiety.

Since ADAB and ADDAB are single- and double-chained analogues of each other, comparison of the self-assembling behaviour of the two surfactants can be used to determine the affect of addition of a second hydrocarbon chain.

Both ADAB [7, 8, 12] and ADDAB [9–11, 34] have been studied previously and polymerised at low concentrations in both isotropic solution (i.e., below the critical micelle (cmc) or critical vesicle concentration (cvc), respectively) and in their aggregated state as micelles or vesicles. Both γ irradiation and thermal initiation using an added initiator were utilised, with the two methods giving conflicting results. The work performed here is an extension of these studies, including the full phase behaviour of the surfactants and their attempted polymerisation.

Experimental

Materials

Allyldodecyldimethylammonium bromide (ADAB, $CH_3–(CH_2)_{11}–N^+(CH_3)_2(CH_2–CH=CH_2)Br^-$), was prepared in the same manner as described by Paleos et al. [7]. Elemental Analysis: Calculated for $C_{17}H_{36}NBr$:C 61.08%; H 10.78%; N 4.19%; Br 23.95%. Found C 61.58%; H 10.88%; N 3.85%; Br 23.69%. m.p. 74 °C. NMR Analysis: Proton $C\underline{H}_3–(CH_2)_{11}$ 0.86 δ; $CH_3–(C\underline{H}_2)_8$ 1.23 δ; $CH_3–(CH_2)_8–C\underline{H}_2$ 1.32 δ; $C\underline{H}_2–CH_2–N$ 1.73 δ; $(C\underline{H}_3)_2–N$ 3.36 δ; $CH_2–C\underline{H}_2–N$ 3.50 δ; $=CH–C\underline{H}_2–N$ 4.38 δ; $C\underline{H}_2=C$ doublet of doublets centred at 5.75 δ; $C\underline{H}=CH_2$ 5.96 δ. Carbon 13 $\underline{C}H_3–CH_2$ 14.02 δ; $CH_3–\underline{C}H_2$ 22.58 δ; $\underline{C}H_2–CH_2–N$ 22.73 δ; $\underline{C}H_2–(CH_2)_2–N$ 26.23 δ; $CH_3–(CH_2)_2–\underline{C}H_2$ 29.15 δ; $CH_3–(CH_2)_3–(\underline{C}H_2)_5$ 29.50 δ; $CH_3–CH_2–\underline{C}H_2$ 31.82 δ; $(\underline{C}H_3)_2–N$ 50.42 δ; $N–\underline{C}H_2–(CH_2)_{10}$ 63.84 δ; $C–\underline{C}H_2–N$ 65.96 δ; $C=\underline{C}H_2$ 124.44 δ; $\underline{C}H=CH_2$ 129.96 δ. FTIR

© Steinkopff Verlag 1996

Analysis: C=C stretch 1467.1 cm^{-1}; H–C= stretch 3015.6 cm^{-1}.

Allyldidodecylmethylammonium bromide (ADDAB, $(CH_3–(CH_2)_{11})_2–N^+(CH_3)(CH_2–CH=CH_2)Br^-$) was used from two sources; it was purchased from SOGO Pharmaceutical Co., Ltd., but also had to be prepared using the standard method [9, 10, 34, 35] due to limited availability of the surfactant from SOGO. Elemental Analysis: Calculated for $C_{28}H_{58}NBr$: C 68.82%; H 11.96%; N 2.87%; Br 16.35%. Found C 68.73%; H 11.90%; N 2.83%; Br 16.54%. m.p. 72 °C. NMR Analysis: Proton $C\underline{H}_3–(CH_2)_{11}$ 0.87 δ; $CH_3–(C\underline{H}_2)_8$ 1.24 δ; $CH_3–(CH_2)_8–C\underline{H}_2$ 1.34 δ; $C\underline{H}_2–CH_2–N$ 1.70 δ; $C\underline{H}_3–N$ 3.32 δ; $CH_2–C\underline{H}_2–N$ 3.39 δ; $=CH–C\underline{H}_2–N$ 4.34 δ; $C\underline{H}_2=C$ doublet of doublets centred at 5.7 δ; $C\underline{H}=CH_2$ 5.9 δ. Carbon 13 $\underline{C}H_3–CH_2$ 14.56 δ; $CH_3–\underline{C}H_2$ 22.91 δ; $\underline{C}H_2–CH_2–N$ 23.11 δ; $\underline{C}H_2–(CH_2)_2–N$ 26.80 δ; $CH_3–(CH_2)_2–\underline{C}H_2$ 29.77 δ; $CH_3–(CH_2)_3–(\underline{C}H_2)_5$ 29.90 δ; $CH_3–CH_2–\underline{C}H_2$ 32.34 δ; $\underline{C}H_3–N$ 48.82 δ; $N–\underline{C}H_2–(CH_2)_{10}$ 61.44 δ; $C=\underline{C}H_2–N$ 61.44 δ; $C=\underline{C}H_2$ 124.60 δ; $\underline{C}H=CH_2$ 130.26 δ. FTIR Analysis: C=C stretch 1465.4 cm^{-1}; H–C= stretch 3003.7 cm^{-1}.

α,α'-Azobis(isobutyronitrile) (AIBN, $(CH_3)_2C(CN)N=N(CN)C(CH_3)_2$), extra pure, was purchased from Tokyo Kasei Kogyo Co., Ltd. and further purified by recrystallisation from methanol.

Techniques

Proton and carbon 13 nuclear magnetic resonance (NMR) spectra were obtained using a Varian VXR300S spectrophotometer operating at 25 °C. Samples were prepared in $CDCl_3$ using tetramethylsilane as an added reference.

D_2O deuterium quadrupolar NMR studies, performed on the liquid crystalline phases of the ADDAB/D_2O system, were accomplished by using a modified Varian XL 100-15 pulsed spectrometer working in the Fourier transform mode using an external lock and operated at a resonance frequency of 15.351 MHz.

Electrical conductivity measurements were obtained by using a TPS Conductivity Meter Model 2102A (Auto-Ranging, Auto Cell, K factor) which was calibrated by using standard potassium chloride solutions (0.1 M KCl, conductivity 1.290×10^{-2} $S \cdot cm^{-1}$ and 1×10^{-3} M KCl, conductivity 1.471×10^{-4} $S \cdot cm^{-1}$). All samples were equilibrated at 25 ± 0.1 °C.

Surface tension measurements were performed by using a tensiometer where a platinum du Noüy ring was employed. The surface tension was determined from the maximum force exerted on the ring without detachment of the menicus [36, 37]. All samples were equilibrated at 25 ± 0.1 °C.

All phase behaviour was investigated initially by polarising optical microscopy using the isothermal concentration gradient method [38]. An Olympus BH-2 polarising optical microscope with a Mettler FP82HT hot stage attached to a Mettler FP80HT Central Processor capable of temperature control to ± 0.1 °C was used. The temperature range was between 20° and 90 °C for the various surfactant/water systems studied. Bulk samples were prepared by adding weighed amounts of the surfactant and purified water into a glass ampoule which was flame sealed. The samples were homogenised by continual heating (< 90 °C) and centrifugation over a period of several weeks. Bulk samples of a given composition were also viewed under crossed polarising filters (where all samples were sealed by using Eccobond* 286, a general purpose epoxy adhesive purchased from W.R. Grace and Co.) and the temperature was varied between 20° and 100 °C. Photographic work was obtained with an Olympus C-35 camera that was fitted onto the microscope.

The structure of the liquid crystalline phases was verified by small-angle x-ray scattering (SAXS) measurements using a Kiessig camera [39] with point collimation. All diffraction patterns were recorded on x-ray sensitive film (CEA Reflex 25, double coated high speed film for direct x-ray exposure purchased from CEA AB Sweden). The camera was capable of recording simultaneously both small-angle (sample to film distance of 200 or 400 mm) and wide-angle (film placed in the range of 40 to 70 mm) scattering detection. The camera was attached to a Philips generator 1120/00 with either a ^{60}Co (K_α line with $\lambda = 1.79285$ Å) fine focus high intensity source PW2216/20 using an iron filter or a Cu (K_α line with $\lambda = 1.54439$ Å) fine focus high intensity source PW2213/20 using a nickel filter.

Samples used for x-ray analysis were loaded into thin walled x-ray transparent capillaries of internal diameter 0.7 or 1.0 mm which were sealed. Bulk samples were also sealed between two mica windows, resulting in an approximate sample thickness of 1 mm. Powder diffraction patterns obtained using all three of the different methods to house the sample were identical (apart from reflexions due to the mica windows).

All polymerisations were performed using free radical initiation. Two techniques were employed; thermal initiation of an added initiator (AIBN, a water insoluble initiator which becomes integrated into the hydrocarbon region of the surfactant liquid crystalline phases) and ultraviolet radiation leading to direct decomposition of the monomer. Samples polymerised with the first method were prepared by adding AIBN in a fixed mole ratio to the

surfactant, whereas samples to be initiated by direct decomposition of the monomer had no added initiator. Samples were made up to the correct compositions by adding the appropriate amount of solvent (water in the case of polymerisation in liquid crystalline media and chloroform for polymerisation in a non-aggregated state). Prior to sealing, the ampoules were degassed by the freeze–pump–thaw technique (to remove as much oxygen (a polymerisation inhibitor) as possible) until a constant pressure was obtained through one complete cycle. They were then flame sealed while still under vacuum. Samples containing no added initiator were equilibrated in a manner identical to that explained above, whereas those containing added AIBN were equilibrated by repeated centrifugation and agitation at room temperature to ensure that the extent of polymerisation prior to equilibration of the samples was minimised.

Thermal polymerisations were performed between 45° and 60 °C, depending upon the stability of the samples, in a thermostated water bath or oven (temperature control to $\pm$ 1 °C). Photochemical polymerisations were performed in a photochemical reaction chamber (built in-house) using broad band emission UV lamps (of type NEC-FL8BL, λ centred at 360 nm). This wavelength was chosen, instead of the more conventional 254 nm due to absorption of light of this wavelength by the ampoules used to house the samples. UV initiated polymerisations were conducted in a temperature controlled environment at 30 $\pm$ 1 °C. Both thermal and photochemically initiated polymerisations were stopped by removal of the samples from the reaction environment followed by rapid cooling.

The polymerisation's progress was monitored as a function of time by preparing a number of samples all having the same composition and stopping the polymerisations at the desired times. The extent to which polymerisation took place was determined by performing proton NMR on the samples which had been previously freeze dried to remove all solvent. Upper limits on the molecular weight of the produced polymers was obtained from dialysis.

Results

Critical micellar/vesicular concentration

Figure 1 shows the curve obtained from surface tension measurements of aqueous ADAB solutions at 25 °C. Aggregation of the surfactant molecules was detected by the change in slope and subsequent plateau of the experimental curve. For the ADAB/water system a polynomial of degree three, having a correlation coefficient equal to 0.997, was an adequate fit to the data points obtained prior

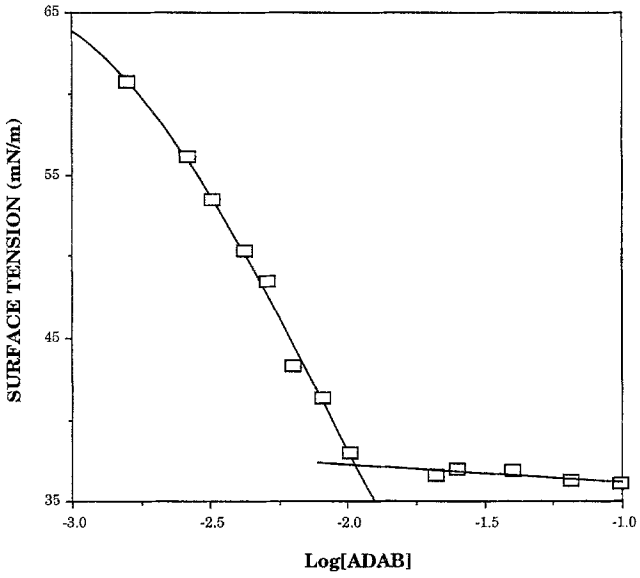

Fig. 1 Surface tension of the ADAB/water system measured by the du Noüy ring method at 25 °C. Errors in the measurements are indicated by the size of the data points

to the concentration at which aggregation occurred. By using this fit, the cmc was determined to be equal to 1.08×10^{-2} M. The surface excess concentration ($\Gamma_2^1 = 2.9 \pm 0.1 \times 10^{-3}$ mol·cm^{-2}) was determined from the slope of the pre-micellisation curve close to the cmc [40–44]. This value yielded an area per polar head group at the interface (A) equal to 58 $\pm$ 1 Å^2.

The electrical conductivity curve obtained for ADAB in water at 25 °C is shown in Fig. 2. The curve shows a distinct break at a concentration of 1.20×10^{-2} M ADAB corresponding to the initiation of surfactant aggregation, in good agreement with the value obtained from surface tension measurements.

The values determined for the cmc of ADAB using both specific conductivity and surface tension measurements compare favourably with the value obtained by Paleos et al. [7] (cmc (ADAB) = 1.25×10^{-2} M, at 25 °C) using electrical conductivity measurements.

For a uni-univalent surfactant a monodisperse mass action-model may be used in conjunction with the conductivity data to determine the percentage dissociation (β) [45–47], assuming that at each concentration there is exclusively an average micelle. It is necessary within this model to use either an experimentally determined value of the aggregation number (n) or an approximation based on the head group area determined from surface tension measurements. Surface tension measurements give the area per head group at the interface as 58 Å^2 therefore the calculated aggregation number is 52 and the percentage dissociation 26.9%. If instead the ratio of the slopes of the

© Steinkopff Verlag 1996

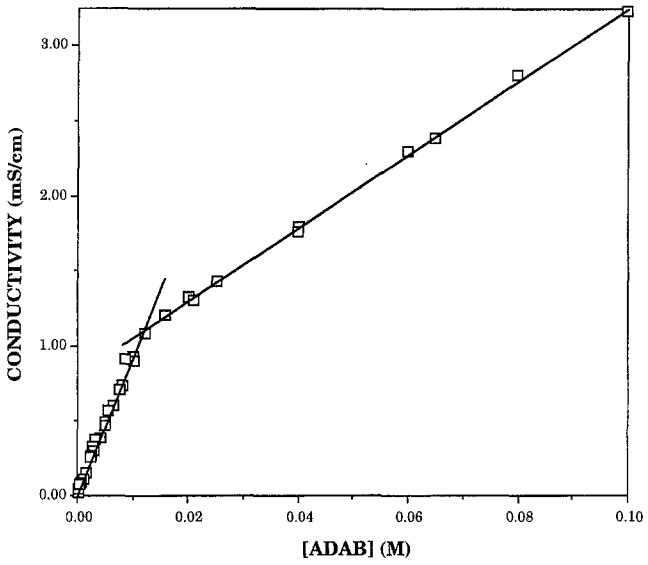

Fig. 2 Electrical conductivity of ADAB measured at 25 °C, the size of the data points indicates the order of the errors in the measurements

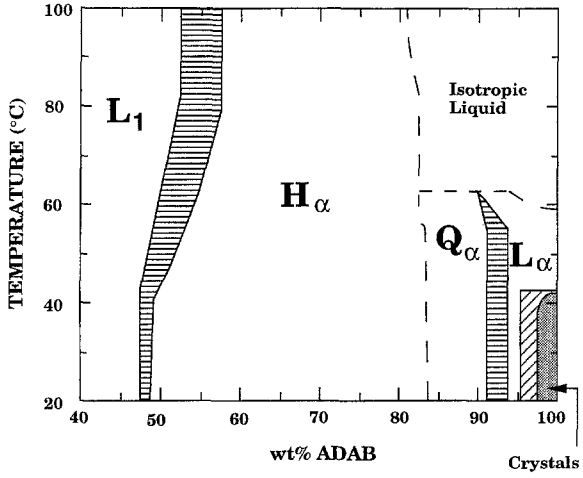

Fig. 3 Partial binary phase diagram of the ADAB/water system. L_1: micellar solution, H_α: hexagonal phase, Q_α: bicontinuous cubic phase (type Q^{230}, Ia3d or Gyroid IPMS), L_α: lamellar phase, Isotropic fluid: random packing of surfactant aggregates, and crystals: hydrated ADAB crystals. Horizontally shaded areas (showing tie lines) indicate regions where two liquid crystalline phases coexist, diagonally shaded areas indicate regions where a liquid crystalline phase coexists with hydrated crystals of ADAB and dashed lines indicate either a weakly first order or second order phase transition

two linear regions of the conductivity curve is used the percentage dissociation is calculated to be 27.2%. Hence, approximately 27% of all bromide counterions dissociate upon micellisation.

Both conductivity and surface pressure-area isotherm measurements were performed with ADDAB in an attempt to determine the surfactant's cvc and head group area. Conductivity measurements were irreproducible; probably due to inaccuracies introduced through loss of surfactant from adsorption to the vessel walls. This is a consequence of the very low concentration at which vesicles are first formed in the ADDAB/water system ($\sim 10^{-6}$ M). In the surface pressure-area isotherm measurements, the monolayer was found not to collapse due to ADDAB being too water soluble. Hence, the cvc and head group area at low concentrations of ADDAB could not be determined by these techniques.

Self-assembly of ADAB

The self-assembly behaviour for the ADAB/water system is shown, by way of a schematic diagram, in Fig. 3. At 20 °C, after formation of a micellar phase (L_1, which exists as a one phase region up to 47.5 wt% ADAB) the system undergoes a first order phase transition yielding a normal hexagonal phase (H_α) existing over a wide temperature and concentration range (48.8 to 83.4 wt% ADAB). When a composition of 83.4wt% ADAB is reached a cubic phase (Q_α) forms. No two phase region was observed between the hexagonal and cubic phases indicating that the transition is either weakly first order or second order. The cubic phase is then transformed into a normal lamellar phase (L_α) following a first order phase transition yielding a pure L_α phase at 94.1 wt% ADAB. As the temperature is increased the lamellar phase melts to give an isotropic fluid whose structure is unknown but is most probably a highly concentrated reverse micellar phase. At higher compositions the L_α phase coexists with hydrated ADAB crystals (the extent and number of these crystalline hydrates was not investigated).

The texture shown in Fig. 4 is one typical of the hexagonal phase of the ADAB/water system and is observed with both concentration gradients and bulk samples. This texture, often termed the "fan texture" [48, 49], is observed when the primary axes of the hexagonal cylinders lie parallel to the glass slide [50]. Note that the curvature of the cylindrical aggregates varies discontinuously about the line disclination of order $s = +1/2$, as evidenced by the splaying out of the brushes of the fan, indicating that the cylinders are relatively limited in their length scale compared with the size of the defect. Regions of the texture also bear a resemblance to the striations analysed by Rogers and Winsor for the hexagonal phase formed by the Tabacco Mosaic Virus [51]. The hexagonal phase is extremely stable to changes in composition and temperature and is very viscous. The cubic phase melts to

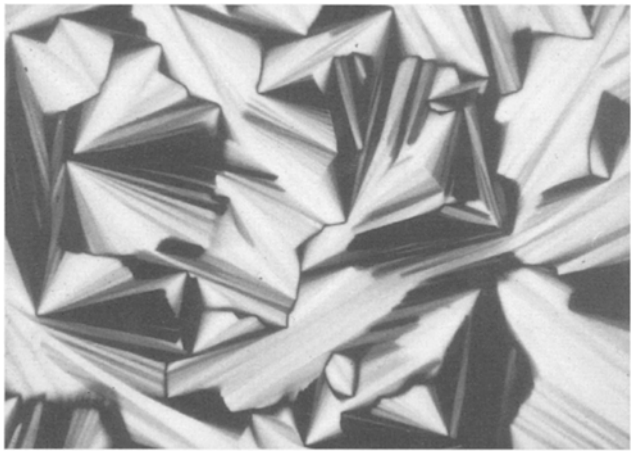

Fig. 4 Optical texture observed for the ADAB hexagonal phase (75.7 wt% ADAB, 30 °C, crossed polarising filters, magnification 240). Cylinders lie parallel to the glass slide and the brushes correspond to line disclinations of strength $s = +1/2$. Note that the brushes of the fans are splayed corresponding to the discontinuous curvature of the hexagonal cylinders about the line disclinations

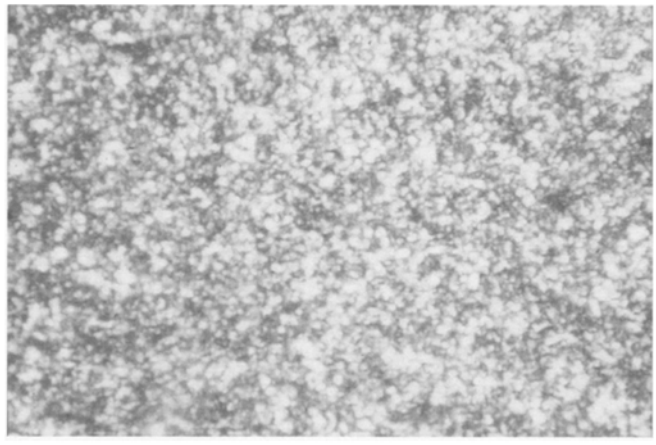

Fig. 5 Mosaic texture of the ADAB lamellar phase (crossed polarising filters, magnification 240). The layers comprising the phase lie parallel to the glass slide (95.1 wt% ADAB sample at 45 °C)

an isotropic fluid at 62.8 °C and its compositional range is reduced compared with that of the hexagonal phase.

A typical "mosaic" texture [48, 52–54] observed for the ADAB lamellar liquid crystalline phase from both bulk samples and concentration gradients is shown in Fig. 5. The texture yields little information on the underlying surfactant geometry and is formed due to the sample adopting a homeotropic orientation on the glass slide. The lamellar phase, like the cubic phase, has reduced stability with respect to increases in temperature compared with that of the hexagonal phase and forms over a very narrow composition range.

The phase behaviour in the ADAB/water system was confirmed by using SAXS. Diffraction patterns were obtained for powdered bulk samples in each of the mesophases of the ADAB/water system and were comprised of Debye–Scherrer rings which were produced by all domains in the irradiated volume.

Samples within the micellar region of the ADAB/water system produced one diffuse ring at small-angles upon irradiation with x-rays (Table 1) and also one diffuse ring ($Q = 1.4\,\text{Å}^{-1}$) at wide angles, indicative of fluid-like chains (this was also found to be the case for the hexagonal, cubic and lamellar phases). These diffraction patterns are typical for randomly distributed micellar aggregates [55].

Diffraction patterns obtained in the small-angle region for the hexagonal liquid crystalline phase of ADAB consisted of from three to five Debye–Scherrer rings which were in the ratio of $1:\sqrt{3}:\sqrt{4}:\sqrt{7}:\sqrt{9}$ (Table 1) as expected for parallel cylinders packed in a two-dimensional hexagonal array.

The ADAB cubic phase is characterised by up to four sharp rings at small-angles with spacings in the ratios of $\sqrt{6}:\sqrt{8}:\sqrt{14}:\sqrt{16}$. These ratios being characteristic of one cubic phase only, the Ia3d (type I, space group 230), which is assumed here to be bicontinuous as has been shown in other systems and is also know as the Gyroid infinite periodic minimal surface (IPMS) [23, 56–61]).

The diffraction pattern for the lamellar phase of ADAB is comprised at small-angles of four sharp rings having Q values in the ratios of 1:2:3:4. This pattern is characteristic of a layered structure.

From the locations of the Bragg peaks the unit cell dimensions were calculated [55]. Structural parameters for the different liquid crystalline phases formed in the ADAB/water system are given in Table 1. All calculations were determined for $T = 27\,°\text{C}$ unless otherwise stated. The specific volume of the hydrocarbon chains was used in all calculations since that of the surfactant is unknown.

From calculations of the head group area in the various ADAB mesophases it is seen that as the concentration of the surfactant increases the amount of water taken up by the head groups of the surfactant as water of hydration decreases, as does the electrostatic interactions between the head groups. This leads to a subsequent decrease in the head group area, such that the head group never increases through a phase transition [55].

Self-assembly of ADDAB

A consequence of ADDAB having two hydrocarbon chains is that the geometries that it can adopt are restricted. The surfactant parameter v/al, where l is the length of the hydrocarbon chain, a is the area per polar

© Steinkopff Verlag 1996

Table 1 Structural parameters determined for the ADAB/water mesophases at $T = 27°C$

ADAB % (w/w)	Phase	Observed Q ($Å^{-1}$)	Unit cell length (a) (Å)	Volume fraction Φ	Paraffin chain thickness (d_s) (Å)	Water and head group thickness (d_w) (Å)	Mean area per polar head (A) ($Å^2$)	hkl
40.0	L_1	0.166	–	0.24	–	–	–	
48.3[a]	L_1	0.145	–	0.29	–	–	–	
53.9	H_α	0.168	43.3	0.32	25.6	17.6	54.8	$10\bar{1}0$
		0.289						$11\bar{2}0$
		0.335						$20\bar{2}0$
		0.443						$21\bar{3}0$
56.1	H_α	0.171	42.5	0.33	25.7	16.9	54.7	$10\bar{1}0$
		0.297						$11\bar{2}0$
		0.341						$20\bar{2}0$
59.9	H_α	0.175	41.4	0.35	25.8	15.6	54.5	$10\bar{1}0$
		0.302						$11\bar{2}0$
		0.345						$20\bar{2}0$
		0.461						$21\bar{3}0$
		0.526						$30\bar{3}0$
69.6	H_α	0.186	39.1	0.40	26.1	13.0	53.8	$10\bar{1}0$
		0.320						$11\bar{2}0$
		0.373						$20\bar{2}0$
		0.488						$21\bar{3}0$
80.5	H_α	0.191	38.1	0.46	27.1	10.9	51.7	$10\bar{1}0$
		0.330						$11\bar{2}0$
		0.380						$20\bar{2}0$
87.1	Q_α (Ia3d)	0.206	74.9	0.50	–	–	–	211
		0.236						220
		0.312						321
88.4	Q_α (Ia3d)	0.211	73.0	0.50	–	–	–	211
		0.244						220
		0.322						321
		0.342						400
90.4	Q_α (Ia3d)	0.213	72.1	0.51	–	–	–	211
		0.244						220
95.0	L_α	0.208	30.2	0.54	16.1	14.0	43.5	001
		0.415						002
		0.623						003
		0.821						004

[a] Temperature 8 °C.

head group at the interface and v is the volume, [62–64] is approximately equal to one and the surfactant should, in principle, spontaneously form mesophases built with bilayers as the fundamental building blocks.

Figure 6 shows the partial phase diagram for the binary system of ADDAB in water. Two liquid crystalline phases are formed between 20° and 100 °C, both consisting of bilayers as their fundamental building blocks. At concentrations below 3.2 wt% ADDAB, an isotropic fluid (L) is formed which due to the double-chained nature of the surfactant is most probably comprised of vesicles. As the concentration is increased the vesicular phase is found to coexist with a birefringent phase consisting of bilayers intercalated with large water regions (L_χ). At 20 °C, this birefringent phase exists as a single phase between 8.8 and 42.7 wt% ADDAB. At ADDAB compositions above 76.1 wt% a normal lamellar phase is formed (planar bilayers intercalated with water, L_α) which melts to give an isotropic fluid at 57.8 °C. Between 42.7 and 76.1 wt% ADDAB the two lamellar phases coexist. It should be noted that the density of these phases differ markedly, with L_χ being denser than both L and L_α.

Evidence consistent with the coexistence of two distinct lamellar phases was obtained by performing deuterium quadrupolar NMR studies upon samples prepared with deuterated water [65–75]. Note that changing the solvent from H_2O to D_2O may have an affect on the phase boundaries of the different liquid crystalline phases observed in the ADDAB/water system but the observed phase progression should not be altered (i.e., both the L_χ and L_α phases should still be formed and transform via a first order phase transition).

Figure 7 shows the spectra obtained for some characteristic regions of the phase diagram shown in Fig. 6. Full

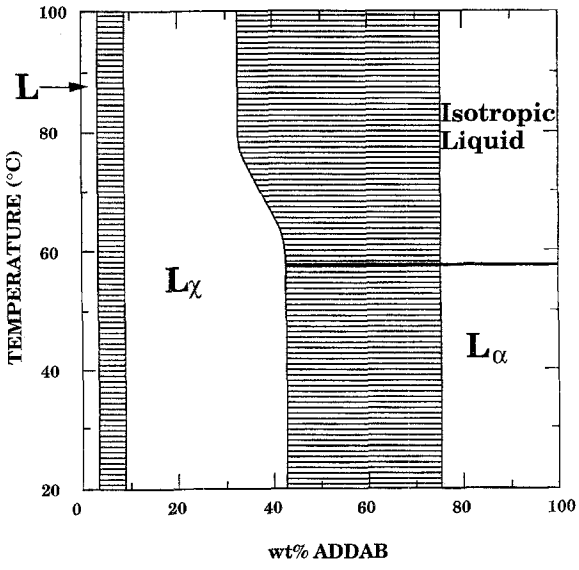

Fig. 6 Binary phase diagram of the ADDAB/water system, L: low concentration isotropic fluid (vesicular phase), L_χ: dilute lamellar phase, L_α: normal lamellar phase, and Isotropic Liquid: randomly distributed surfactant aggregates. Horizontally shaded areas indicate regions where two liquid crystalline phases coexist

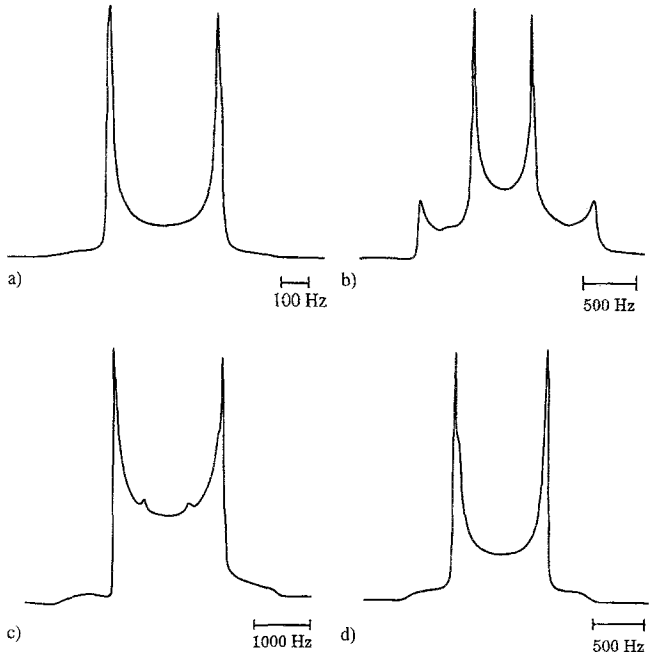

Fig. 7 D_2O deuterium quadrupole NMR spectra for the binary ADDAB/D_2O system at 25°C. a) 35.0 wt% ADDAB (one phase, L_χ), b) 60.2 wt% ADDAB (two phase region, $L_\chi + L_\alpha$), c) 75.6 wt% ADDAB (two phase region, $L_\chi + L_\alpha$), d) 89.3 wt% ADDAB (one phase, L_α)

Table 2 Structural parameters for the ADDAB/water system at 27 °C

ADDAB % (w/w)	Phase	Observed Q (Å^{-1})	Unit cell length (a) (Å)	Volume fraction Φ	Paraffin chain thickness (d_s) (Å)	Water and head group thickness (d_w) (Å)	Mean area per polar head (A) (Å^2)	hkl
24.1	L_χ	0.066	95.1	0.20	19.0	76.1	74.0[a]	001
		0.132						002
		0.198						003
		0.264						004
		0.330						005
35.0	L_χ	0.092	68.7	0.28	19.6	49.1	71.8[a]	001
		0.183						002
		0.274						003
		0.363						004
40.4	L_χ	0.094	66.8	0.33	21.8	45.0	64.5[a]	001
		0.186						002
		0.279						003
		0.375						004
		0.466						005
		0.556						006
80.2	L_α	0.211	29.7	0.61	18.1	11.6	77.6	001
		0.423						002
		0.634						003
		0.841						004
97.0	L_α	0.251	25.0	0.72	18.0	7.0	78.2	001
		0.501						002
		0.746						003

[a] Calculated assuming infinite flat bilayers.

© Steinkopff Verlag 1996

splitting results are shown in Fig. 8. From these results it is indicated that a first order phase transition between the L_χ and L_α phases occurs. In addition, information on the underlying global geometry can also be obtained. The value of the measured quadrupole splitting is dependent upon the interaction of the phase with the applied magnetic field. This overall interaction is comprised of three individual components which are due to [76]:

(a) the average orientation of the surfactant mesophase,

(b) the variation of the orientation of the D_2O molecules at the interface, and

(c) the variation of the orientation of the surfactant molecules in the aggregate (i.e. the curvature of the interface).

For a powder sample the first contribution is a constant and the second variation is averaged out. Hence, the quadrupole splitting within a given surfactant/D_2O system is determined by the extent of curvature of the surfactant aggregates [76]. For example, the normal hexagonal phase has a quadrupole splitting of approximately a factor two less than the corresponding lamellar phase splitting which is a direct consequence of the curvature inherent in the surfactant aggregates of the hexagonal phase as compared with the planar bilayers of the lamellar phase [70]. Therefore, in the case of the L_χ and L_α phases of the ADDAB/D_2O system where the quadrupole splitting of the L_α phase is approximately a factor three greater than in the L_χ phase (in the two phase region, see Fig. 8) this is consistent with the contention that the L_χ phase has a relatively high degree of curvature compared with the L_α phase and cannot be described as consisting of planar bilayers. Note that the measured value of approximately 1750 Hz for the L_α phase is comparable with that of other planar bilayer lamellar phases [74].

Figure 9 shows the optical textures observed during a 30 °C concentration gradient. This photograph shows that an isotropic phase is initially formed which then transforms into a birefringent phase at higher surfactant compositions producing a texture which is atypical for normal lamellar phases (L_α) consisting of planar bilayers. How this texture correlates with the underlying geometry of the surfactant molecules will be discussed later. It should be noted though that as the concentration of surfactant increases (from left to right in the figure) the texture is initially one of maltese crosses (which are spherical on average) superimposed with one to three dark concentric circles and becomes comprised of elongated crosses which finally become completely drawn out. Since this texture has been produced during a concentration gradient, where the molecules are easily oriented by the constrictions imposed on them by the glass slide and cover slip during

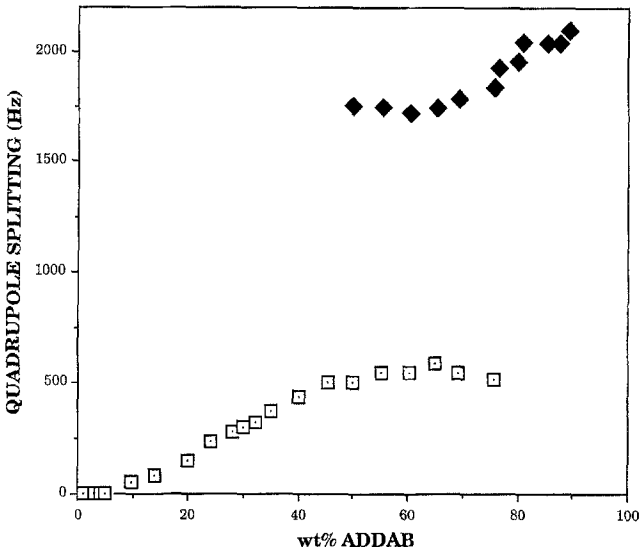

Fig. 8 D_2O deuterium quadrupolar NMR splitting for the ADDAB/D_2O system at 25 °C, errors are indicated by the size of the data points

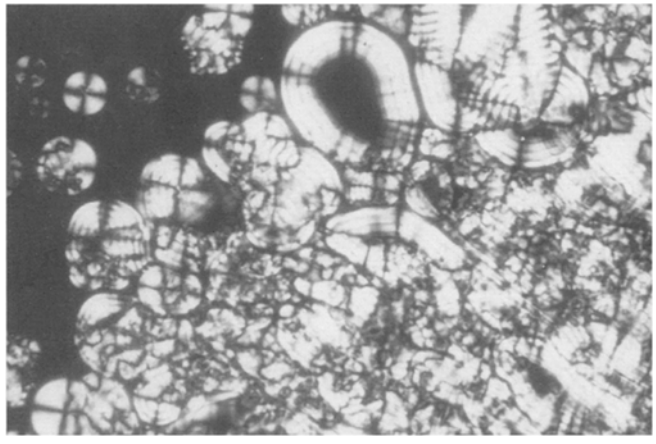

Fig. 9 30 °C concentration gradient of the ADDAB/water system viewed under crossed polarised light, magnification 240. The variation in the texture observed with increase in concentration (left to right) shows the formation of the lower ADDAB composition lamellar phase (L_χ). Note the maltese crosses which are superimposed with dark concentric circles

formation of the liquid crystalline phases, more information is usually able to be obtained from the optical textures produced under these conditions than from a texture observed from a bulk sample where orientational ordering has not been imposed during the growth of the phase. This supposition is supported by the optical texture shown in Fig. 10 under crossed polarising filters for a 25.3 wt% ADDAB sample (L_χ phase). Here the information observed for this phase in Fig. 9 is almost completely lost with only one or two individual maltese crosses being

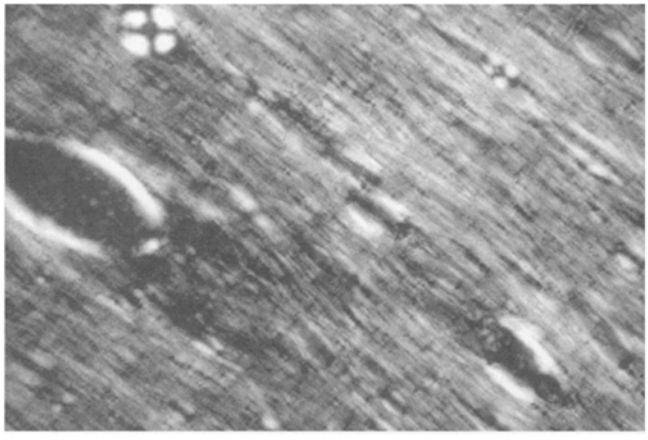

Fig. 10 Texture observed for a bulk sample of the low ADDAB composition lamellar phase (L_χ, 25.3 wt% ADDAB, 30°C, crossed polarising filters, magnification 240). Note the individual maltese crosses which are visible and the superimposed dark concentric circles

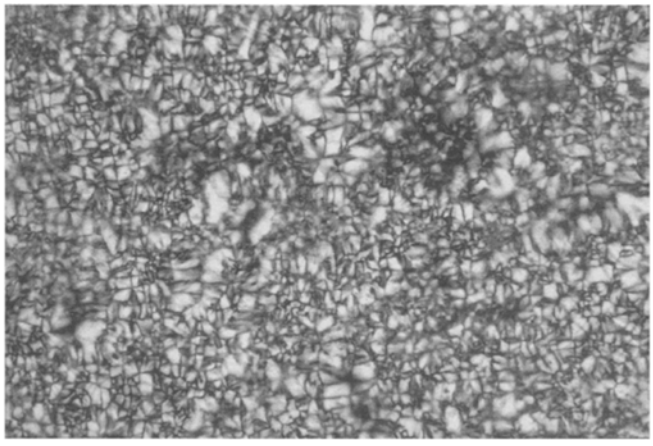

Fig. 11 Mosaic texture of the ADDAB normal lamellar phase (L_α, crossed polarising filters, magnification 240). The layers comprising the phase lie parallel to the glass slide (85.3 wt% ADDAB sample at 35°C)

evident, though it is still possible to discern the superimposed concentric dark bands. Again, the texture is not typical of a normal planar bilayer lamellar phase. This dilute lamellar phase is also found to be of low viscosity and is highly coloured/iridescent when bulk samples are viewed through crossed polarising sheets, indicating that there may be some microcrystalline order which is comparable to the wavelength of light.

In contrast, the texture shown in Fig. 11 for a bulk sample in the L_α phase of the ADDAB/water system (85.3 wt%, 35 °C) is a typical mosaic texture often observed for normal lamellar phases consisting of planar bilayers intercalated with water in a homeotropic orientation with both positive and negative units [48] being apparent (compare with the texture observed for the L_α phase of ADAB, Fig. 5).

The optical microscopy and D_2O deuterium quadrupole NMR results suggest that the lamellar phase formed at low ADDAB concentrations (L_χ) does not consist of planar bilayers intercalated with water where the low concentration lamellar phase is a mere dilution of the highly concentrated phase.

As further evidence for the existence of two distinct birefringent phases whose fundamental building blocks are bilayers, SAXS measurements were performed to determine the structures of the phases. Samples in both birefringent phases gave diffraction patterns comprised of Debye–Scherrer rings which were produced by all domains in the irradiated volume.

The ADDAB low concentration lamellar phase (L_χ) is characterised by a series of sharp rings at small-angles with Q values in the ratios of 1:2:3:4:5:6. Similarly in the high composition lamellar phase (L_α) the small-angle diffraction pattern consists of Bragg peaks in the ratios of 1:2:3:4. Despite both lamellar phases giving rise to diffraction patterns consistent with normal planar bilayers (i.e., Bragg peaks in the ratio of 1:2:3 ...) calculation of the head group area of the two phases assuming infinite flat bilayers (which is the major assumption made for calculation of head group areas of a lamellar phase) shows that the head group area actually increases during the phase transition from L_χ and L_α. An increase in head group area with increase in surfactant concentration leading to a phase transition is unlikely [55]. This suggests that the lower composition lamellar phase may not be comprised of infinite planar bilayers; consistent with the results obtained from both optical microscopy and D_2O deuterium quadrupole NMR. An interpretation of these results will be given later. Table 2 gives the structural parameters calculated for the two lamellar liquid crystalline phases formed in the ADDAB/water system. All calculations were determined for $T = 27$ °C, the specific volume of the hydrocarbon chains was used in all calculations.

Polymerisation of monomeric ADAB and ADDAB

Attempts to polymerise both ADAB and ADDAB in an isotropic state, in order to characterise the polymers self-assembly and compare it with that observed for the monomeric form, were unsuccessful using both thermal initiation via AIBN (up to 10 mol% to surfactant) and photochemical irradiation (where the surfactant was dissolved in chloroform at a concentration of 0.25 M). Exposure times ranged from 1 day to 2 weeks. ADDAB was

Colloid & Polymer Science, Vol. 274, No. 4 (1996)
© Steinkopff Verlag 1996

found to polymerise to less than 5% whereas, although, ADAB polymerised to approximately 30% it was also found to decompose during the polymerisation (solutions became bright yellow and NMR analysis showed that the integrity of approximately 5% of the surfactant was not maintained during the polymerisation). Attempted purification of polymeric ADAB was unsuccessful and unfortunately no further work could be performed on the polymeric forms of ADAB or ADDAB.

Polymerisation of liquid crystalline phases

The polymerisation of the two different lamellar phases (25 and 85 wt% ADDAB, L_χ and L_α, respectively) of the ADDAB/water system was investigated. As for the isotropic polymerisation of ADDAB, polymerisation of the liquid crystalline phases formed by this surfactant was unsuccessful using both thermal and photochemical initiation over a time period of from 1 day to 4 weeks. Hence, there was no enhancement of the extent of polymerisation due to favourable alignment of the surfactant molecules imposed by the liquid crystalline phase geometry.

In the ADAB/water system five regions from the phase diagram were chosen for polymerisation, corresponding to the dilute and concentrated regions of the micellar phase (5 and 40 wt% ADAB), the hexagonal phase (65 wt% ADAB), the cubic phase (88 wt% ADAB) and the lamellar phase (95 wt% ADAB). Thermal initiation was activated at 50 °C due to the cubic and lamellar phases melting at approximately 60 °C. No problems due to the surfactant self-initiating during equilibration of the liquid crystalline phases was experienced.

Table 3 shows the percentage conversions for the five regions of the ADAB/water phase diagram activated by thermal initiation of added AIBN (10 mol% to surfactant). The corresponding results for photochemical initiation are given in Table 4.

These results indicate that polymerisation which has been activated either thermally via an added initiator or photochemically give almost identical results, i.e., there is no influence by the type of initiation on the extent to which polymerisation occurs. There is also no trend of increasing polymerisation with time for either form of initiation. All samples polymerise to approximately 30% which is comparable with the results obtained for polymerisation in an isotropic state in chloroform. Therefore, as well as the type of initiation having no influence on the extent of polymerisation, the packing of the surfactant molecules does not change the yield of the polymer formed. It should be noted that the higher ADAB composition phases were found to decompose during polymerisation when activated thermally (solutions became bright yellow or orange and NMR analysis showed that the integrity of

Table 3 Percentage conversions for the five regions from the ADAB/water phase diagram polymerised thermally

Time (days)	Low weight percent micellar solution	High weight percent micellar solution	Hexagonal phase	Cubic phase	Lamellar phase
0.25	–	–	–	27.6	24.8
0.5	20.5	–	–	30.9	28.5
0.75	–	–	–	24.3	32.2
1	30.2	–	22.0	–	21.2
2	26.1	21.2	16.3	11.6	–
2.125	–	–	–	25.2	19.1
3.125	–	–	–	23.5	21.6
4	24.1	24.1	27.6	33.2	31.4
6	–	23.0	23.1	–	–
7	24.5	25.2	–	30.8	29.3
7.125	24.7	21.6	25.9	–	–
8	–	–	–	32.9	21.6
9	–	–	–	27.5	31.6
10	18.0	17.5	22.4	–	–
11	–	–	20.0	–	–
12	20.4	18.6	26.1	27.0	–
14	–	–	23.2	–	–
15	26.8	–	–	37.1	17.0
17	–	–	–	33.3	32.4
18	28.4	–	18.1	–	–
20	16.1	20.4	24.0	–	–
22	–	–	–	37.2	39.4
24	25.6	30.0	21.5	35.0	38.0
28	29.6	26.3	24.2	–	–
31	24.2	25.2	–	–	–

Table 4 Percentage conversions for the five regions of the ADAB/water phase diagram polymerised photochemically

Time (days)	Low weight percent micellar solution	High weight percent micellar solution	Hexagonal phase	Cubic phase	Lamellar phase
0.25	–	–	–	33.5	32.6
0.5	–	–	–	30.0	27.1
0.75	–	–	–	33.1	–
1	33.2	22.7	33.6	27.3	–
1.5	–	–	–	26.0	–
2	21.4	29.1	25.5	28.0	26.6
4	23.2	23.9	29.5	28.1	27.8
6	–	–	–	22.7	36.9
8	24.7	36.7	36.2	–	28.7
10	–	–	–	33.5	24.6
11	33.7	30.8	34.0	–	–
16	33.2	28.1	35.5	–	–
19	29.6	31.4	28.7	–	–

approximately 5% of the surfactant was not maintained during the polymerisation).

To determine if the underlying surfactant geometry was maintained during the polymerisation, SAXS experiments were performed on the samples after polymerisation had occurred. All samples studied were initiated photochemically, due to the decomposition of the samples during thermal initiation, and were exposed to irradiation for a period of 2 days.

Samples in the concentrated micellar region were found to produce diffraction patterns having one diffuse ring only at both small- and wide-angles. Comparison with the diffraction pattern obtained for a monomeric sample (Table 1) shows that there is little difference between the average distance between the micellar aggregates in the partially polymerised and non-polymerised systems. Hence, formation of the ADAB polymer had little affect on the characteristics of the micellar solution.

In contrast, the hexagonal, cubic and lamellar phases all showed in conjunction with the sharp Bragg peaks attributable to non-polymerised ADAB, retaining the original monomeric surfactant geometry, two inner diffuse rings. Calculation of structural parameters for what is assumed to be a structure now comprised of a non-polymerised surfactant matrix interwoven with polymer chains is given in Table 5. Unit cell lengths and head group areas for the different phases were calculated by assuming that the non-polymerised surfactant forming the hexagonal, cubic or lamellar matrix retains the original ratio of surfactant to water during the polymerisation. Comparison of the calculated values for the partially polymerised systems (Table 5) with the monomeric values (Table 1) shows that the presence of the interwoven polymer chains throughout the monomeric matrix has not disturbed significantly the packing of the surfactant molecules. Indeed, it has been determined that both the cubic and lamellar phases have an increased stability of approximately 20 °C due to the presence of the interwoven polymer chains and that the textures observed for the birefringent phases are comparable to those observed when no polymer was present. Figures 12 and 13 show the optical textures for the partially polymerised hexogonal and lamellar phases, respectively. These figures can be compared with the optical textures observed for the non-polymerised phases (Figs. 4 and 5). Although the polymer has not been fully incorporated into the monomeric matrix (i.e., the surfactant molecules have not maintained their original geometry) polymerisation has increased the stability of the phases significantly.

Discussion

ADAB

Incorporation of the allyl polymerisable moiety into a single-chain quaternary ammonium surfactant has been found to have a considerable effect upon the surfactant's self-assembling behaviour.

From electrical conductivity and surface tension results for ADAB (cmc $= 1.1 \pm 0.1 \times 10^{-2}$ M, $\beta =$ 27%, $A = 58 \pm 1$ Å^2, $\Gamma_2^1 = 2.9 \pm 0.1 \times 10^{-6}$ mol·m^{-2}) and its non-polymerisable analogue DTAB (cmc $= 1.5 \pm 0.1 \times 10^{-2}$ M, $\beta = 34\%$, $A = 49 \pm 1$ Å^2, $\Gamma_2^1 = 3.4 \pm 0.1 \times 10^{-6}$ mol·m^{-2}) [26] it can be shown that addition of the allyl group changes the interactions between the surfactant molecules. The concentration at which aggregation begins, the extent of dissociation of the bromide counterions and the surface excess concentration are all decreased slightly while the head group area is increased significantly. The interactions between the surfactant molecules are more favourable due to the presence

© Steinkopff Verlag 1996

Table 5 Structural parameters for the polymeric liquid crystalline phases of ADAB at $T = 27°C$

ADAB % (w/w)	Phase	Observed Q ($Å^{-1}$)	Unit cell length (a) (Å)	Volume fraction Φ	Paraffin chain thickness (d_s) (Å)	Water and head group thickness (d_w) (Å)	Mean area per polar head (A) ($Å^2$)	hkl
40.0	L_1	0.153	–	0.24	–	–	–	
63.1	H_α	0.069[a]						
		0.120[a]						
		0.178	40.8[b]	0.37[b]	26.0[b]	14.8[b]	54.0[b]	$10\bar{1}0$
		0.307						$11\bar{2}0$
		0.355						$20\bar{2}0$
90.0	Q_α	0.074[a]						
	(Ia3d)	0.130[a]						
		0.203	75.7	0.51	–	–	–	211
		0.234						220
		0.312						321
95.0	L_α	0.081[a]						
		0.142[a]						
		0.213	29.5[c]	0.54[c]	15.8[c]	13.7[c]	44.5[c]	001
		0.425						002
		0.635						003

[a] Diffuse inner rings due to interwoven polymer chains.
[b] Calculated assuming that the remaining monomeric surfactant forming the hexagonal phase is still at a composition of 63.1 wt%.
[c] Calculated assuming that the remaining monomeric surfactant forming the lamellar phase is still at a composition of 95.0 wt%.

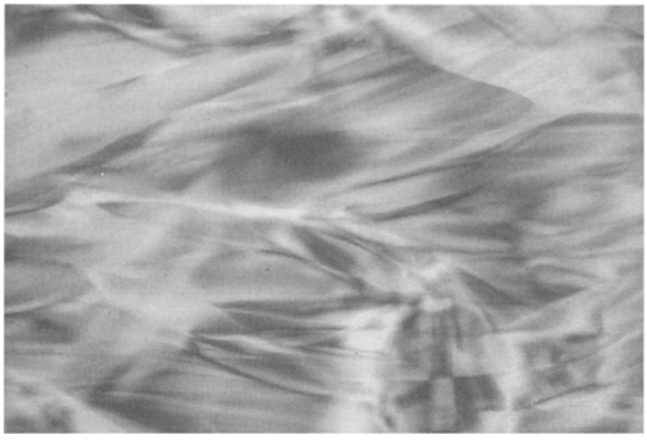

Fig. 12 Optical texture observed for the partially polymerised ADAB hexagonal phase (63.1 wt% ADAB, 30°C, crossed polarising filters, magnification 240). Note that the sample is more highly disordered (compare with Fig. 4)

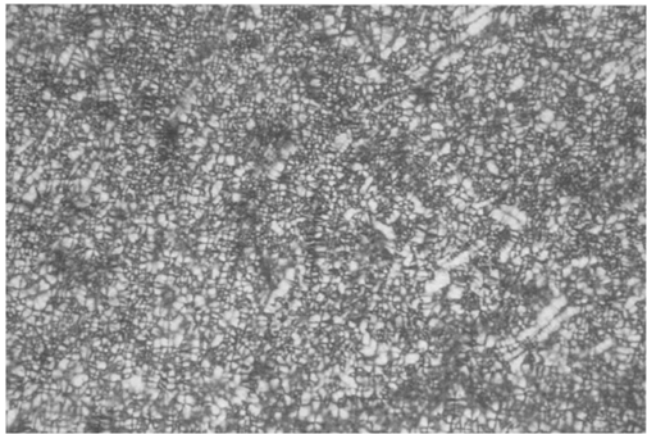

Fig. 13 Mosaic texture of the partially polymerised ADAB lamellar phase (crossed polarising filters, magnification 240). The layers comprising the phase lie parallel to the glass slide (95.0 wt% ADAB sample at 25°C, compare with Fig. 5)

of the allyl group, which also induces a slight reduction in the overall charge of the micellar aggregates (i.e., the allyl group, in effect reduces the electrostatic interactions between the head groups of the amphiphiles which is important since this interaction is one of the dominant interactions to be overcome during polymerisation).

Not only is the aggregation at low concentrations influenced by this change in the nature of the surfactant but indeed the self-assembly over all surfactant compositions is altered. Comparison of the phase diagrams for the ADAB/water system (Fig. 3) and the DTAB/water system [26] (Fig. 14) shows that the presence of the allyl group induces an increase in the solubility of the surfactant in water but a corresponding decrease in the stability of the concentrated liquid crystalline phases that are formed. Note that with ADAB the concentrated phases are accessible at room temperature. This significant change can only be attributed to the presence of the allyl

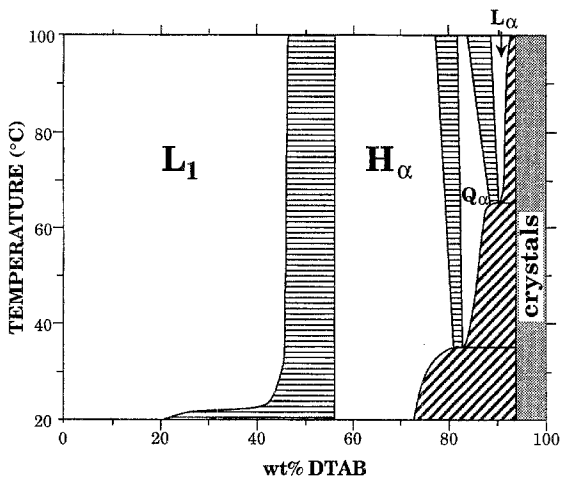

Fig. 14 Partial phase diagram of the binary DTAB/water system [26]. L_1: micellar solution, H_α: normal hexagonal phase, Q_α: bicontinuous cubic phase, type Q^{230} (Ia3d-Gyroid IPMS [31, 52, 53, 93–95]), L_α: lamellar phase, and crystals: hydrated DTAB crystals. The horizontally shaded areas (showing tie lines) indicate a region where two liquid crystalline phases coexist and the diagonally shaded areas indicate coexistence between a liquid crystalline phase and hydrated crystals

polymerisable group, which changes the overall rigidity, hydrophilicity and charge of the head group. These naturally affect both the head group area and the length and flexibility of the hydrocarbon chain, since, both of these parameters are strongly influenced by the extent of hydration and counterion binding. Therefore, even a seemingly small change to the nature of the surfactant, by way of replacing a methyl group with an allyl group, can significantly alter the balance of the interactions between amphiphiles.

Why is the extent to which polymerisation occurs in both isotropic and self-assembled forms so low?

It has been shown [77–83] that polymerisation of unsaturated non-amphiphilic quaternary ammonium compounds is extremely difficult and that thermal polymerisation in acqueous solution using water soluble initiators is not possible for monomers containing only one allyl group.

Results obtained here show that it is possible to polymerise a quaternary ammonium surfactant containing one allyl group either in chloroform (where the surfactant is not self-assembled but does have a preferential alignment) or in water in a self-assembled state, where the extent of polymerisation in all cases is approximately 30%. Addition of a hydrocarbon chain, introducing an amphiphilic nature and allowing the molecules to align preferentially, enables polymerisation to occur. The extent of polymerisation is still, however, very low due to the intrinsic resistance to polymerisation of the allyl group and its placement near the charged centre of the surfactant. It was found that increasing the length of the reaction time did not increase the extent of polymerisation, therefore, polymerisation is very rapid and reaches a plateau almost immediately.

The reason for the low conversion must be a consequence of:

(a) the rate constant for formation of a free radical from the allyl monomer being slow and/or the activation barrier being very high (note that this is now also influenced by the nearness of the electrostatic centre),

(b) recombination to form the original carbon–carbon double bond prior to propagation is favourable (i.e. the time required for reformation of the original carbon–carbon double bond is not sufficient for a second carbon–carbon double bond to be found in the correct orientation for propagation to occur), and

(c) the rate constants for the termination reactions are faster than those for the propagation steps.

Therefore, the molecular weight of these polymers is expected to be low, this has indeed been found; molecular weights of the polymers formed using either thermal or photochemical initiation from self-assembled or isotropic states were less than 8000 as determined from dialysis experiments.

Paleos et al. [7, 8, 12] have shown that polymerisation of ADAB both above and below its cmc by using thermal initiation (added AIBN) and γ irradiation gave conflicting results. It was stated that by using γ irradiation, polymerisation was effective within 48 h (with the extent of polymerisation increasing with time) at a dose rate of 2300 rad·min^{-1}. Polymerisation of an isotropic solution by γ irradiation lead to complete decomposition of the surfactant whereas in the micellar state no decomposition occurred and molecular weight determinations showed that the average polymer chain contained approximately 30 monomer units, compared with a maximum of 20 determined here for all self-assembled and isotropic forms. In contrast, polymerisations with thermal initiation gave irreproducible results and were abandoned [7, 8, 12]. These results are incommensurate with both the results obtained here and those observed in the study by Butler et al. [77–83]. Also the large increase in the extent to which polymerisation occurs when γ irradiation is used was not explained. A brief trial, performed here, using γ irradiation on micellar solutions of ADAB showed that decomposition occurred to a large extent and no polymerisation was detected.

In this study, polymerisation of the liquid crystalline phases of the ADAB/water system was found to induce neither phase separation nor phase transformation. The unpolymerised monomer retained its original geometry with slight variations to the repeat distance and head

Colloid & Polymer Science, Vol. 274, No. 4 (1996)
© Steinkopff Verlag 1996

group areas due to accommodation of the interwoven polymer. This polymer was incorporated throughout the monomer matrix and its presence lead to an increase in the stability of the liquid crystalline phases.

ADDAB

The addition of a second chain to the surfactant alters drastically the preferred geometric packing of the surfactant molecules from one where the system forms highly curved interfaces (as observed in the ADAB/water system where micellar, hexagonal and cubic phases are formed) to that of relatively planar interfaces. This preferential packing is mirrored in the determined phase diagram where the only self-assembled aggregates found to form in the ADDAB/water system are built using bilayers as their fundamental units.

What exactly is the progression in the geometric packing of the surfactant molecules with increase in surfactant concentration in the ADDAB/water system?

From the experimental results earlier the two lamellar phases observed in the ADDAB/water system are not necessarily related in the sense that the low composition lamellar phase (L_χ) is a mere dilution of the high composition lamellar phase (L_α). It is considered that both phases locally are comprised of bilayers of surfactant intercalated with water with the more concentrated phase showing all the characteristics of a "normal" lamellar phase were the bilayers are assumed to be parallel, infinite and flat but a different global surfactant packing must be assigned to the low composition phase.

Bellare et al. [84] have simulated the polarised microscope images produced for a series of surfactant geometries. In one simulation a lamellar type phase having a relatively high degree of curvature (i.e., a structure resembling a multi-walled vesicular type phase or so called "onion" phase) is generated where the number of bilayers comprising the structure is altered. The computed images of these generated structures range from the traditional maltese cross to maltese crosses superimposed with concentric dark bands (these being observed when the spacing between the layers is smaller than twice the discretisation spacing of the computer program). In the case of a real system the number of dark bands superimposed on the maltese crosses relates indirectly to the number of bilayers in the multi-walled aggregates as long as the spacing between the bilayers is neither too long nor too short. From Fig. 9, therefore, it may be deduced that the surfactant aggregates formed are probably a construction of multi-layered bilayers with a relatively high degree of curvature. It is not possible to determine the number of bilayers in each aggregate from the observed texture since, the dark bands do not directly correspond to the bilayers (the length scale being of the order of 10^3 times different between the observed texture and the underlying surfactant geometry).

This idea of the L_χ phase being comprised of curved surfactant aggregates based on surfactant bilayers is supported by the results obtained from D_2O deuterium quadrupole NMR and SAXS experiments.

The phase progression for the ADDAB/water system below 57.8 °C may be postulated to involve initially the formation of a normal vesicular phase (L) at very low surfactant concentrations where the vesicles are comprised of a single bilayer and are on average spherical. As the concentration is increased the vesicles remain spherical but begin to be the composite of more than one bilayer, i.e., "nesting" occurs [85]. Spherical nesting cannot continue indefinitely and eventually the spherical shape of the onion begins to distort and the average aggregation number increases giving a pure one phase region (L_χ). This phase may consist of a multi-walled elongated structure similar to a multi-walled ribbon structure, where the ribbons here are based on bilayers and not on a solid surfactant packing as in the usual case. The local structure of the phase may be bilayers intercalated with large quantities of water but globally the bilayers are not infinite and flat. The contention is that the phase is a completely separate and unique thermodynamic liquid crystalline phase and can, therefore, coexist with a second normal lamellar phase (L_α), which is formed at higher compositions. The viscosities of the two phases are also found to be very different, the first being of extremely low viscosity whereas the high composition lamellar phase has a viscosity comparable with other normal lamellar phases. At temperatures about 57.8 °C the normal lamellar phase is no longer stable and an isotropic fluid is formed.

The coexistence of two essentially lamellar phases in double-chain surfactant/water systems has been previously observed by a number of groups [27–29, 33, 72, 86, 87] and theoretically predicted by Wennerström [88, 89] and Jönsson and Perrson [90]. One of the systems in which the formation of two lamellar phases has been observed is the non-polymerisable analogue of ADDAB, DDAB. The observation of two distinct lamellar phases which coexist in this system was first reported by Fontell et al. [27] and then later by Warr et al. [28] before a more complete phase diagram was published by Zemb et al. [33] in 1993. This diagram is reproduced in Fig. 15.

Comparison of the two phase diagrams for the ADDAB/water system (Fig. 6) and the DDAB/water system (Fig. 15) reveals, as in the case of ADAB versus DTAB, both similarities and differences which can be attributed to the presence of the allyl group. The major difference between these two phase diagrams is the presence of a critical

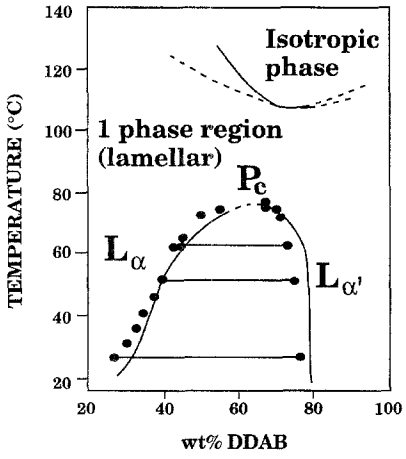

Fig. 15 Partial phase diagram of the binary DDAB/water system, courtesy of Zemb et al. [33]. L_α: collapsed lamellar phase with a periodicity of 32 Å including the thin water layer (6 Å), $L_{\alpha'}$: swollen lamellar phase which can be diluted with water up to 3% DDAB content. P_c is the critical point. The two phase region between the lamellar and the isotropic phase present at higher temperatures is too narrow to be determined experimentally (following Zemb et al. [33] Fig. 1)

point in the DDAB/water system, above which a one phase lamellar region is observed (i.e., a lamellar phase which is continuous with increase in surfactant concentration). Whereas below the critical point two distinct lamellar phases are observed to exist and there is a region where a discontinuous transformation between the two occurs (i.e., the two phases coexist). At higher temperatures an isotropic phase is found. From reported electron micrographs [30, 31, 33] the two distinct DDAB lamellar phases appear to have a global surfactant geometry which are very similar to those found in the ADDAB/water system. It appears that the low composition phase is not comprised of parallel infinite flat bilayers, unlike the high composition phase, but instead the bilayers have a curvature associated with them forming multi-walled structures. At temperatures below the critical point the free energy curve has two local minima allowing these two phases to coexist. As the temperature is increased the free energy curve no longer allows for the formation of two distinct phases and a continuous transformation is observed with the multi-walled aggregates of the low composition lamellar phase (L_α in Fig. 15, L_χ in the ADDAB/water system, Fig. 6) continuously transforming with increase in composition to finally be consistent with parallel infinite flat bilayers. Therefore, x-ray analysis both above and below the critical point should show a continuous and discontinuous variation (as was observed in the ADDAB/water system) in all determined surfactant parameters as the concentration of DDAB is increased, respectively.

The critical point phenomenon is not observed in the ADDAB/water system and, in comparing the two phase diagrams, it can be imagined that the ADDAB/water phase diagram may be obtained from the DDAB/water phase diagram by shifting the formation of the isotropic phase to lower temperatures (i.e., in effect reducing the stability of the high composition lamellar phase).

The reduction in the stability of the high composition liquid crystalline phase to changes in temperature upon addition of the allyl group to the head group of a surfactant was also observed in the ADAB/water system when compared with the DTAB/water system. The increased flexibility introduced into the head group of the surfactants upon replacement of a methyl with an allyl group leads to a decrease in the stability of the phases to changes in temperature. Therefore, a one phase continuous transition with increasing surfactant concentration is never observed in the ADDAB/water system due to this change in the intrinsic rigidity moduli of the surfactant.

Addition of the allyl polymerisable group to both single- and double-chain surfactants has been shown to induce similar changes in the observed self-assembly of the surfactant. Although the general phase behaviour for the surfactants is maintained (i.e., both the single- and double-chain surfactants show phase behaviour which is comparable with that of non-polymerisable surfactants of the same class), the allyl group has the effect of producing subtle changes so that the aggregates formed behave differently to changes in composition and temperature to those observed when the group is not present.

The viscosities of the phases formed are also found to be effected by the presence of the allyl group and in general there is a decrease in the viscosity of the phases.

Comparison of the ADAB/water and ADDAB/water phase behaviour shows that the change in the surfactant parameter on addition of the second hydrocarbon chain is the significant influence on the self-assembly of the surfactants.

Why is polymerisation in the double-chained surfactant not possible whereas the single-chain analogue has been shown to polymerise to approximately 30% in both isotropic and self-assembled forms?

Any difference between the polymerisability of the two surfactants must be due to the presence of the second hydrocarbon chain in ADDAB. It has been shown [91, 92] that the second paraffinic chain in double-chain surfactants adopts the conformation where the first two or three carbon atoms lie parallel to the hydrophilic/hydrophobic interface. Adoption of this conformation will lead to an increased steric interaction between the surfactant molecules. This will be accomodated by an increased separation between the surfactant molecules and head group area in the liquid crystalline phases formed (see Table 2). The

Colloid & Polymer Science, Vol. 274, No. 4 (1996)
© Steinkopff Verlag 1996

increase in the distance between two allyl groups caused by the configuration adopted by the second chain will decrease the rate constant for the propagation steps giving the free radical (which has already in the case of ADAB been shown to be difficult to generate) an increased time for reformation of the original carbon–carbon double bond. This is in addition to the increased hindrance to propagation of polymerisation caused by the added steric interaction. In the case of the single allyl group, where initiation is difficult and termination is faster than propagation, this increased interaction is sufficient to stop polymerisation occurring other than to an extent of approximately 5%.

Babilis et al. [9–11], have reported that polymerisation of ADDAB in its vesicular form by γ irradiation is possible to 100% in approximately 5 h at a dose rate of 1850 rad·min^{-1}. Again as was the case for ADAB earlier, γ irradiation was found to be more efficient than catalytic polymerisation induced by AIBN. Precipitation was shown to occur during polymerisation which the authors have attributed to probable destruction of the surfactant monomer. It was also stated that ADDAB, which follows the same polymerisation mechanism as ADAB, was found to polymerise more readily than the single-chain surfactant which was stated to be due to favourable placements of the monomers in the vesicles. This contrasts with the results obtained here, which show that ADDAB polymerisation did not occur. The reasons for the differences in the results obtained for γ irradiation where polymerisation to 100% is observed versus thermal and photochemical initiation where polymerisation does not occur are presently unknown.

Conclusions

It has been shown that replacement of a methyl group in the head group region of a single- and a double-chain quaternary ammonium surfactant by an allyl polymerisable group changes the hydrophilicity and rigidity of the head group. It also introduces changes in the electrostatic interactions between the surfactant molecules, the solubility of the surfactant in water (making the high composition liquid crystalline phase more readily accessible) and the stability of the phases formed.

Photochemical and thermal polymerisation of the allyl group in this position of the surfactant was difficult to induce and did not occur in the double-chain surfactant. Where polymerisation did occur the liquid crystalline phases for the ADAB/water system were found to neither phase separate nor undergo a phase transformation during polymerisation. The unpolymerised monomer retained its original geometry with slight variations to the repeat distance and head group areas due to accommodation of the interwoven polymer, which is incorporated throughout the monomer matrix and leads to an increase in the stability of the liquid crystalline phases.

Therefore incorporation of the allyl polymerisable moiety into the head group of a single-chain quaternary ammonium surfactant and subsequent polymerisation increased the accessibility of the high composition liquid crystalline phases and also their stability to changes in temperature.

Acknowledgments This work was begun while CJD was a visiting scientist at The Australian National University and the recipient of a Queen Elizabeth II Fellowship from the Australian Research Council. Some of the preliminary work for these systems was also done while CJD was a visiting scientist at Physical Chemistry 1, University of Lund, Sweden. The assistance of Ali Khan and the late Krister Fontell during this initial period is gratefully acknowledged. KMM was the recipient of an Australian Postgraduate Research Award. We also thank Patrick Kékicheff and Stephen Hyde for useful discussions and Monique Dubois for allowing reproduction of the DDAB phase diagram.

References

1. Herz J, Reiss-Husson F, Rempp P, Luzzati V (1964) J Polym Sci: Part C 4:1275–1290
2. Friberg S, Thundathil R, Stoffer J (1979) Science 205:607–608
3. Larrabee Jr C, Sprague E (1979) J Polym Sci: Polym Lett Ed 17:749–751
4. Thundathil R, Stoffer J, Friberg S (1980) J Polym Sci: Part A: Polym Chem Ed 18:2629–2640
5. Sprague E, Duecker D, Larrabee Jr C (1981) J Am Chem Soc 103:6797–6800
6. Fendler J, Tundo P (1984) Acc Chem Res 17:3–8
7. Paleos C, Dais P, Malliaris A (1984) J Polym Sci: Part A: Polym Chem Ed 22:3383–3391
8. Paleos C, Dais P (1984) In: Vhapory C (ed) Recent Advances in Liquid Crystalline Polymers. Elsevier, London, pp 89–95
9. Babilis D, Dais P, Margaritis L, Paleos C (1985) J Polym Sci: Part A: Polym Chem Ed 23:1089–1098
10. Babilis D, Dais P, Paleos C (1985) Polym Prepr (Am Chem Soc Div Polym Chem) 26:206–207
11. Babilis D, Paleos C, Dais P (1988) J Polym Sci: Part A: Polym Chem Ed 26:2141–2156
12. Paleos C, Malliaris A (1988) Rev Macromol Chem Phys C28:403–419
13. Ringsdorf H, Scharb B (1988) Makromol Chem 189:299–315
14. Anderson D, Ström P (1989) In: El-Nokayl M (ed) Polymer Association Structures: Microemulsions and Liquid Crystals. American Chemical Society, Washington, DC, pp 204–224
15. Ström P (1992) J Colloid Interface Sci 154:184–193

16. Ström P, Anderson D (1992) Langmuir 8:691–709
17. Cochin D, Candau F, Zana R (1993) Macromolecules 26:5755–5764
18. Cochin D, Zana R, Candau F (1993) Macromolecules 26:5765–5771
19. Denton J, Duecker D, Sprague E (1993) J Phys Chem 97:756–762
20. Glatzhofer D, Cho G, Lai L, O'Rear E, Fung B (1993) Langmuir 9:2949–2954
21. Kurja J, Nolte R, Maxwell I, German A (1993) Polymer 34:2045–2049
22. Luzzati V, Reiss-Husson F (1966) Nature 210:1351–1352
23. Luzzati V, Tardieu A, Gulik-Krzywicki T, Rivas E, Reiss-Husson F (1968) Nature 220:485–488
24. Blackmore E, Tiddy G (1988) J Chem Soc, Faraday Trans II 84:1115–1127
25. Fontell K (1990) Colloid Polym Sci 268:264–285
26. McGrath K (1995) Langmuir 11: 1835–1839
27. Fontell K, Ceglie A, Lindman B, Ninham B (1986) Acta Chem Scand A 40:247–256
28. Warr G, Sen R, Evans D, Trend J (1988) J Phys Chem 92:774–783
29. Dubois M, Zemb T (1991) Langmuir 7:1352–1360
30. Dubois M (1991) Cristaux liquides lamellaires lyotropes gonfles: Utilisation de la microstructure comme milieu reactif de gelification inorganique. Thesis 3° cycle, A L'Université Paris XI Centre D'Orsay
31. Dubois M, Gulik-Krzywicki T, Cabane B (1993) Langmuir 9:673–680
32. Zemb T, Belloni L, Dubois M, Marcelja S (1992) Prog Colloid Polym Sci 89:33–38
33. Zemb T, Gazeau D, Dubois M, Gulik-Krzywicki T (1993) Europhys Lett 21:759–766
34. Paleos C, Margomenou-Leonidopoulou G, Babilis D, Christias C (1987) Mol Cryst Liq Cryst 146:121–135
35. Ralston A, Eggenberger D, du Brow P (1948) J Am Chem Soc 70:977–979
36. du Noüy P (1919) J General Physiology 1:521–524
37. Furlong D, Freeman P, Metcalfe I, White L (1983) J Chem Soc, Faraday Trans I 79:1701–1719
38. Rendall K, Tiddy G, Trevethan A (1983) J Chem Soc, Faraday Trans I 79:637–649
39. Kiessig V (1942) Kolloid Z 98:213–221
40. Haydon D, Phillips J (1958) Trans Faraday Soc 54:698–704
41. Weil I (1966) J Phys Chem 70:133–140
42. Aveyard R, Haydon D (1973) An Introduction to the Principles of Surface Chemistry. Cambridge University Press, London
43. Simister E, Thomas R, Penfold J, Aveyard R, Binks B, Cooper P, Fletcher P, Lu J, Sokolowski A (1992) J Phys Chem 96:1383–1388
44. Lu J, Simister E, Thomas R, Penfold J (1993) J Phys Chem 97:6024–6033
45. Hutchinson E (1954) J Colloid Sci 9:191–196
46. Evans H (1956) J Chem Soc 579–586
47. Kamrath R, Franses E (1984) J Phys Chem 88:1642–1648
48. Rosevear F (1954) J Am Oil Chem Soc 31:628–639
49. Rosevear F (1968) J Soc Cosmetic Chemists 19:581–594
50. Oswald P, Kléman M (1981) J Phys France 42:1461–1472
51. Rogers J, Winsor P (1969) J Colloid Interface Sci 30:500–510
52. Kléman M, Colliex C, Veyssié M (1976) In: Friberg S (ed) Lyotropic Liquid Crystals and the Structure of Biomembranes. American Chemical Society, Washington, DC, pp 71–84
53. Allain M, Kléman M (1987) J Phys France 48:1799–1807
54. Boltenhagen P, Lavrentovich O, Kleman M (1991) J Phys II France 1:1233–1252
55. Luzzati V (1968) In: Chapman D (ed) Biological Membranes: Physical Fact and Function. Academic Press, London, pp 71–123
56. Luzzati V, Spegt P (1967) Nature 215:701–704
57. Scriven L (1976) Nature 263:123–125
58. Scriven L (1977) In: Mittal K (ed) Micellization, Solubilization and Microemulsions. Plenum Press, pp 877–893
59. Fontell K (1981) Mol Cryst Liq Cryst 63:59–82
60. Rançon Y, Charvolin J (1987) J Phys France 48:1067–1073
61. Clerc M, Dubois-Violette E (1994) J Phys II France 4:275–286
62. Israelachvili J, Mitchell D, Ninham B (1976) J Chem Soc Faraday Trans II 72:1525–1568
63. Israelachvili J, Mitchell D, Ninham B (1977) Biochim Biophys Acta 470: 185–201
64. Mitchell D, Ninham B (1981) J Chem Soc Faraday Trans II 77:601–629
65. Cohen M, Reif F (1957) Solid State Phys 5:321–438
66. Stejskal E, Tanner J (1965) J Chem Phys 49:288–292
67. Johansson Å, Lindman B (1974) In: Gray G, Winsor P (ed) Liquid Crystals & Plastic Crystals: Physico–Chemical Properties and Methods of Investigation. Ellis Horwood Ltd Chichester, pp 192–230
68. Luckhurst G (1974) In: Gray G, Winsor P (ed) Liquid Crystals & Plastic Crystals. Physico-Chemical Properties and Methods of Investigation. Ellis Horwood Limited, Chichester, pp 144–191
69. Persson N, Lindman B (1975) J Phys Chem 79:1410–1418
70. Lindblom G, Perrson N, Arvidson G (1976) In: Friberg S (ed) Lyotropic Liquid Crystals and the Structure of Biomembranes. American Chemical Society, Washington, DC, pp 121–141
71. Seelig J (1977) Quart Rev Biophys 10:353–418
72. Khan A, Fontell K, Lindblom G, Lindman B (1982) J Phys Chem 86: 4266–4271
73. Davis J (1983) Biochim Biophys Acta 737:117–171
74. Kékicheff P (1989) J Colloid Interface Sci 131:133–152
75. Henriksson U, Blackmore E, Tiddy G, Söderman O (1992) J Phys Chem 96:3894–3902
76. Kékicheff P (1987) Des cylindres aux bicouches: étude structurale des transformations de phase dans un cristal liquide lyotrope. Thèse d'Etat, Université de Paris-Sud, Centre d'Orsay
77. Butler G, Bunch R (1949) J Am Chem Soc 71:3120–3122
78. Butler G, Ingley R (1951) J Am Chem Soc 73:895–896
79. Butler G, Goette R (1952) J Am Chem Soc 74:1939–1941
80. Butler G, Bunch R, Ingley F (1952) J Am Chem Soc 74:2543–2547
81. Butler G, Goette R (1954) J Am Chem Soc 76:2418–2421
82. Butler G, Angelo R (1956) J Am Chem Soc 78:4797–4800
83. Butler G, Angelo R (1957) J Am Chem Soc 79:3128–3131
84. Bellare J, Davis H, Miller W, Scriven L (1990) J Colloid Interface Sci 136: 305–326
85. Simons B, Cates M (1992) J Phys II France 2:1439–1451
86. Uang Y, Blum F, Friberg S, Wang J (1992) Langmuir 8:1487–1491
87. Ockelford J, Timimi B, Narayan K, Tiddy G (1993) J Phys Chem 97: 6767–6769
88. Wennerström H (1987) In: Meunier J, Langevin D, Boccara N (Ed) Physics of Amphiphilic Layers. Springer-Verlag, Berlin Heidelberg, pp 171–176
89. Wennerström H (1990) Langmuir 6:834–838
90. Jönsson B, Persson P (1987) J Colloid Interface Sci 115:507–512
91. Hitchcock P, Mason R, Thomas K, Shipley G (1974) Proc Nat Acad Sci USA 76:3036–3040
92. Israelachvili J, Marcelja S, Horn R (1980) Quart Rev Biophys 13:121–200
93. Wennerström H, Persson N, Lindman B (1975) ACS Symp Ser 9:253–269
94. McCall D, Douglass D, Anderson E (1963) Ber Bunsenges Phys Chem 67:336–340
95. Bloom M, Davis J, Mackay A (1981) Chem Phys Lett 80:198